

InP Self Assembled Quantum Dot Lasers Grown on GaAs Substrates by Metalorganic Chemical Vapor Deposition

R. D. Dupuis¹⁾, J. H. Ryou^{*1)}, R. D. Heller¹⁾, G. Walter²⁾, D. A. Kellogg²⁾, N. Holonyak, Jr.²⁾, C. V. Reddy³⁾, V. Narayanamurti³⁾, D. T. Mathes⁴⁾, and R. Hull⁴⁾

¹⁾ Microelectronics Research Center, The University of Texas at Austin
10100 Burnet Road, Building 160, Austin, TX 78758 USA

Phone: +1-512-471-0537, Fax: +1-512-471-0957, e-mail: dupuis@mail.utexas.edu

²⁾ Center for Compound Semiconductor Microelectronics, The University of Illinois at Urbana-Champaign, Urbana, IL

³⁾ Gordon McKay Laboratory of Applied Science, Harvard University, Cambridge, MA 02138

⁴⁾ Department of Materials Science and Engineering, The University of Virginia, Charlottesville, VA

*Now with Honeywell VCSEL Products Division, Plymouth MN 55441

ABSTRACT

We describe the operation of lasers having active regions composed of InP self-assembled quantum dots embedded in $\text{In}_{0.5}\text{Al}_{0.3}\text{Ga}_{0.2}\text{P}$ grown on GaAs (100) substrates by MOCVD. InP quantum dots grown on $\text{In}_{0.5}\text{Al}_{0.3}\text{Ga}_{0.2}\text{P}$ have a high density on the order of about $1\text{-}2 \times 10^{10} \text{ cm}^{-2}$ with a dominant size of about 10-15 nm for 7.5 ML growth.[1] These $\text{In}_{0.5}\text{Al}_{0.3}\text{Ga}_{0.2}\text{P}/\text{InP}$ quantum dots have previously been characterized by atomic-force microscopy, high-resolution transmission electron microscopy, and photoluminescence.[2] We report here the 300K operation of optically pumped red-emitting quantum dots using both double quantum-dot active regions and quantum-dot coupled with InGaP quantum-well active regions. Optically and electrically pumped 300K lasers have been obtained using this active region design; these lasers show improved operation compared to the lasers having QD-based active regions with threshold current densities as low as $J_{th} \sim 0.5 \text{ KA/cm}^2$.

INTRODUCTION

III-phosphide self-assembled quantum-dot (SAQD or simply QD) structures having delta-functional behavior of the density of states and the discrete energy levels of carriers induced by three-dimensional quantum confinement offer the potential to realize injection lasers operating in the visible spectral region with improved performance characteristics, such as low threshold current density, high characteristic temperature, and high differential gain [3,4,5]. The direct growth of coherently strained defect-free self-assembled quantum dots on planar substrates using the coherent Stranski-Krastanow (SK) growth mode [6,7] offers the potential to develop QD visible laser devices with the theoretically predicted and experimentally realized improved performance. Also, the SAQD growth process can overcome the limitation of lattice matching between the substrate and epitaxial active region due to the intrinsic strain-compliant nature of the SK growth mode.

III-As quantum dot-related structures for infrared optoelectronic applications at $\lambda \sim 1.3\text{-}1.5 \mu\text{m}$ have been extensively researched for growth condition optimization, material property characterization, and device applications including lasers in the infrared spectral region. Since

the first demonstration of InAs quantum dot lasers [8], a great deal of research on III-As based quantum dot structures have led to quantum-dot lasers with improved threshold current densities and characteristic temperatures [9] as compared to more conventional quantum-well lasers. However, in comparison to the III-As material system, less research has been performed in the development of III-phosphide SAQD structures for applications in the visible-light spectral region. Initially, it was reported that the properties of III-P SAQDs had a reduced QD density and a broader size distribution than those of the III-As SAQDs. Due to the "blue-shift" effect of the emission from the SAQDs induced from multiple orders of quantum confinement and compressive strain on QDs, there is the potential to extend the wavelength of light emitters to the yellow or green spectral regions using binary and ternary III-Phosphide SAQD structures.

In the past, structures with active regions containing InP SAQDs on GaAs substrates, the QDs have generally been grown on $\text{In}_{0.49}\text{Ga}_{0.51}\text{P}$ matrix layers by MBE [10,11], MOCVD [12,13], or by hydride vapor phase epitaxy (VPE) [14]. InP SAQDs embedded in $\text{In}_{0.49}\text{Ga}_{0.51}\text{P}$ grown on GaAs (100) substrates grown by MOCVD have been reported to yield relatively low densities of SAQDs ($\sim 10^7$ - 10^9 cm^{-2}), compared to III-As SAQDs, and a bimodal size distribution of coherent islands has been reported. InP SAQDs have also been grown on GaP substrates [15] to modify the strain applied to InP QDs; however, no PL emission from the QDs was observed, possibly due to the expected Type II conduction band alignments in this system. Moreover, the growth of InP SAQDs is not as well developed as the growth of III-As SAQDs and further investigation is required.

To improve the QD density, the effect of different matrix layers lattice-matched to GaAs substrates having larger bandgap, such as $\text{In}_{0.49}(\text{Al}_x\text{Ga}_{1-x})_{0.51}\text{P}$ ($x=0.3, 0.6, 1.0$), needs to be studied to improve the carrier confinement. Furthermore, a different matrix material system is expected to change the morphology and growth characteristics of the InP SAQDs. Additionally, the matrix material affects the optical properties of SAQD structures. Recently, we studied the growth of InP SAQDs on InAlGaP matrix layers and the effect of coupling quantum dot states with the electronic states of the InGaP quantum well [20,21,22,23].

EXPERIMENT

In the present study, InP SAQD growth conditions are employed which have been optimized with various matrix layers with regards to QD size, uniformity, and density as well as optical quality to fabricate InP QD based laser operating in visible light spectral region with improved characteristics. InP quantum dots coupled to InGaP quantum wells have been studied. These lasers have lased CW optically and pulsed electrically pumped at 77K and 300K. QD material and optical properties are characterized by atomic force microscopy (AFM), photoluminescence (PL), and high-resolution transmission electron microscopy (TEM).

The InAlGaP/InP QD and laser structures in this work were grown by low-pressure metalorganic chemical vapor deposition (MOCVD) in an EMCORE Model GS3200 UTM rotating disk reactor at ~ 60 Torr using a H_2 ambient. The group III precursors used are trimethylindium (TMIn), trimethylaluminum (TMAI), and triethylgallium (TEGa); the group V hydride sources are arsine (AsH_3) and phosphine (PH_3). Disilane (Si_2H_6) is used as a source of Si for *n*-type doping and bis-cyclopentadienyl magnesium (Cp_2Mg) is used for *p*-type (Mg) doping. The growth was performed simultaneously on two-inch diameter GaAs:Si (100) on-axis, (100)- 10° $\langle 111 \rangle$ A, and (100)- 15° $\langle 111 \rangle$ A substrates.

The surface morphology of SAQDs is characterized by tapping-mode AFM on the exposed QD samples to determine the QD average (or dominant) size, density, and uniformity. The QD size is expressed in terms of the height as measured by AFM. The density is taken from the multiple sets of relatively large area AFM scans. To evaluate the morphology, the $\text{In}_{0.5}\text{Al}_{0.5}\text{P}/\text{InP}$ QD structure used consists of an $\text{In}_{0.49}(\text{Al}_x\text{Ga}_{1-x})_{0.51}\text{P}$ lower matrix layer (250 nm thick) followed by an InP QD active layer all grown on a GaAs buffer layer/GaAs:Si (100) substrate. Following the QD deposition, the growth is terminated and the wafer is cooled down under a PH_3 overpressure to prevent desorption. The lattice parameters of the $\text{In}_{0.49}(\text{Al}_x\text{Ga}_{1-x})_{0.51}\text{P}$ ($x=0.3, 0.6, 1.0$) matrix layers are analyzed using a Rigaku high-resolution five double-crystal X-ray diffractometry (using a four-crystal monochromator) to determine the degree of lattice matching to the substrate. For lattice-matched matrix layers, the epitaxial layers are calibrated to have less than ~ 200 arc-seconds of angle separation relative to the GaAs substrate measured from an (004) X-ray rocking curve. This is done in order to minimize the strain effect from the matrix layer on the growth of active QD layer. The optical properties of InP SAQDs embedded in various matrices are characterized by room-temperature and low-temperature PL. For the PL measurements, a ~ 488 nm excitation source from an Ar^+ laser operating at a constant power density (50 – 200 mW) and a GaAs photomultiplier with a GaAs photocathode are used. For these quantum-dot heterostructures (QDHs), the $\text{In}_{0.49}(\text{Al}_x\text{Ga}_{1-x})_{0.51}\text{P}$ upper matrix layer is grown on the InP SAQD layer with a certain post-purge time after the completion of SAQD layer deposition. TEM is also used to study the microscopic morphology and material quality of individual QDs with and without upper matrix layer, as shown in

The InP SAQD growth conditions are optimized by altering the growth temperature, growth time, and V/III ratio. The growth temperature of the QDs is optimized at 650°C for 1 minute (7.5 ML) with a V/III ratio $\sim 2,100$. The estimated nominal growth rate of InP has been reduced to ~ 0.125 monolayer/sec (ML/s), as calibrated by measuring the thickness of a thin InP planar layer using glancing grazing incidence X-ray reflectivity.

METHODS USED

In this study, we report some of the characteristics of the InP SAQDs. We also report the device results of optically and electrically pumped lasers based on these InP SAQDs. The InP QD growth studies are performed by altering growth temperatures and times and using various $\text{In}_{0.49}(\text{Al}_x\text{Ga}_{1-x})_{0.51}\text{P}$ matrices ($x=0.0, 0.3, 0.6$, and 1.0). The morphology changes of the exposed SAQDs depend on the growth time and the matrix material, and are characterized by atomic force microscopy (AFM). Photoluminescence (PL) spectra were taken at 4K and 300K to determine the light-emitting characteristics of the $\text{InP}/\text{In}_{0.49}(\text{Al}_x\text{Ga}_{1-x})_{0.51}\text{P}$ quantum-dot heterostructures (QDHs). 4K PL spectra from the InP SAQDs embedded in $\text{In}_{0.49}(\text{Al}_x\text{Ga}_{1-x})_{0.51}\text{P}$ cladding layers exhibit PL emission in the visible orange and red spectral regions, as shown below. Also, transmission electron microscopy is used to characterize the microscopic material quality and morphology of the individual QD and the interfaces between SAQD and cladding layers.

RESULTS OBTAINED

AFM studies of InP SAQDs grown on InAlGaP matrix layers have shown that under some conditions, a relatively high density of small quantum dots is produced, as described in Figure 1. As the QD growth proceeds with longer deposition times, the average QD height (and

base width) increases and the average density correspondingly decreases. Our work has concentrated on the 7.5ML effective QD thickness where the size and density appear to be optimal for light emitting properties determined by PL.

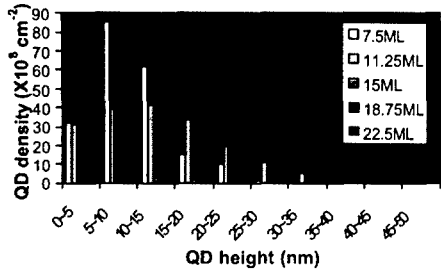


Figure 1: Variation of height and density vs. nominal layer thickness for InP SAQDs.

The 4K PL intensity vs. wavelength spectra for $\text{InP}/\text{In}_{0.49}(\text{Al}_{0.6}\text{Ga}_{0.4})_{0.51}\text{P}$ QDHs grown for different deposition times is shown in Figure 2. The PL spectral peak position changes from 591 nm (2.10 eV for 3.75 MLs), to 653 nm (1.90 eV for 7.5 MLs) and 681 nm (1.82 eV for 15 ML), as the deposition time increases. This PL emission is at a lower energy than that observed from comparable-sized InP QDs embedded in $\text{In}_{0.49}\text{Al}_{0.51}\text{P}$.

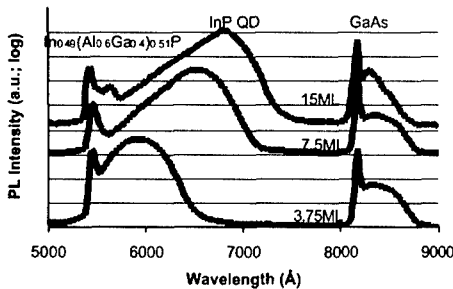


Figure 2: 4K PL spectra of InP SAQDs embedded in InAlGaP cladding layers grown at 650 °C for various deposition times.

However, $\text{InP}/\text{In}_{0.49}(\text{Al}_{0.6}\text{Ga}_{0.4})_{0.51}\text{P}$ QDHs exhibit more efficient luminescence than $\text{InP}/\text{In}_{0.49}\text{Al}_{0.51}\text{P}$ QDHs at room temperature, possibly due to better electron confinement. TEM studies of the InP SAQDs have shown the dislocation-free structure of single- and multiple-layer QDHs and the vertical alignment achieved for multiple QD layers, as shown in Figure 3. These InP QD active regions have been incorporated into various separate-confinement laser active regions. In the present work, we have grown three types of quantum-confined “red-emitting” active region laser structures on GaAs substrates: (1) single- and multiple-QDHs; (2) single-QW active-region QDHs; and couples QD+QW structures and compared the 300K and 77K PL emission, as shown in Figure 4. Recently, we have described the effects of coupling of the InP QD states to the electronic states of InGaP quantum wells grown below and above the quantum dots, resulting in the coupling of the quantum dots through

electronic states in the quantum wells [24]. Optically and electrically pumped 300K lasers using QD+QW active regions have been obtained using this unique design; these lasers show improved operation compared to lasers having QD-based active regions with pulsed 300K threshold current densities $J_{th} \sim 1.5 \text{ KA/cm}^2$, as shown in Figure 5. By optimizing the coupling between the quantum well and the quantum-dots, other QD+QW laser devices have been grown that exhibit pulsed J_{th} values at 300K as low as $\sim 0.5 \text{ KA/cm}^2$.

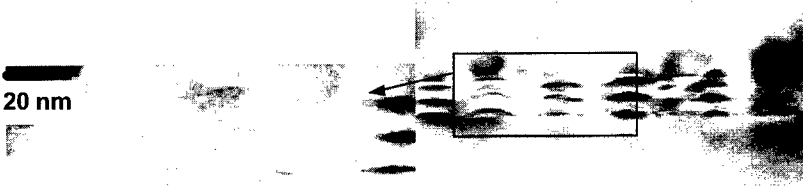


Figure 3: TEM micrograph of stacked InP SAQDs.

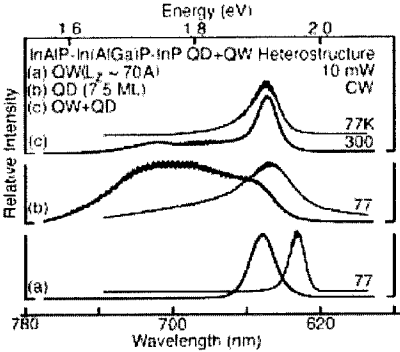


Figure 4: PL spectra for InAlP-InAlGaP-InP QW, QD, QD+QW samples.

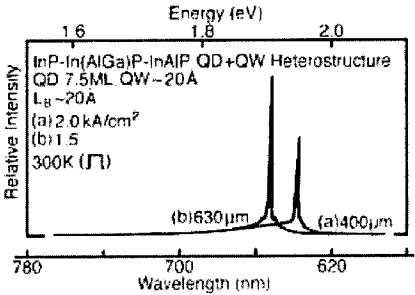


Figure 5 : InAlP-InAlGaP-InP QD+QW 300K electrically pumped optical spectra.

CONCLUSIONS

In summary, we have grown and characterized InP SAQDs embedded in $\text{In}_{0.49}(\text{Al}_x\text{Ga}_{1-x})_{0.51}\text{P}$ matrices ($x=0.0, 0.3, 0.6$, and 1.0). The InP SAQDs grown at 650C exhibit uniform morphology with a 5-10 nm dominant height and $\sim 2 \times 10^{10} \text{ cm}^{-2}$ density for 7.5 ML. As the deposition time increases, the QD size increases, while the density decreases slightly, and the PL peak position shifts to lower energy. For InP/ $\text{In}_{0.5}\text{Ga}_{0.5}\text{P}$ / $\text{In}_{0.49}(\text{Al}_{0.6}\text{Ga}_{0.4})_{0.51}\text{P}$ / $\text{In}_{0.49}\text{Al}_{0.51}\text{P}$ SQD+SQW injection lasers, we have achieved electrically pumped lasing at 681 nm at 300 K with reduced threshold current densities as low as 0.5 KA/cm^2 . We believe this approach is applicable to other QD laser materials systems.

REFERENCES

- [1] J. H. Ryou, R. D. Dupuis, G. Walter, N. Holonyak, Jr., D. T. Mathes, R. Hull, C. V. Reddy, and V. Narayanamurti, *J. Appl. Phys.*, to be published.
- [2] J. H. Ryou, PhD. Dissertation, The University of Texas at Austin (2001).
- [3] Y. Arakawa and H. Sakaki, *Appl. Phys. Lett.* **40**, 939 (1982).
- [4] M. Asada, Q. Miyamoto, and Y. Suematsu, *IEEE J. Quantum Electron.* **QE-22**, 1915 (1986).
- [5] N. N. Ledentsov, M. Grundmann, F. Heinrichsdorff, D. Bimberg, V. M. Ustinov, A. E. Zhukov, M. V. Maximov, Zh. I. Alferov, and J. A. Lott, *IEEE J. Select. Topic. Quantum Electron.* **6**, 439 (2000).
- [6] I. N. Stranski and L. Krastanow, *Akad. Wiss. Wien, Math-Naturwiss. Klasse* **146**, 797 (1937).
- [7] V. A. Shchukin and D. Bimberg, *Rev. Mod. Phys.* **71**, 1125 (1999).
- [8] N. N. Ledentsov, V. M. Ustinov, A. Y. Egorov, A. E. Zhukov, M. V. Maksimov, I. F. Tavatadze, and P. S. Kop'ev, *Semiconductors* **28**, 832 (1994).
- [9] G. Park, O. B. Shchekin, S. Csutak, D. L. Huffaker, and D. G. Deppe, *Appl. Phys. Lett.* **75**, 3267 (1999).
- [10] A. Kurtenbach, K. Eberl, and T. Shitara, *Appl. Phys. Lett.* **66**, 361 (1995).
- [11] A. Kurtenbach, C. Ulrich, N. Y. Jin-Phillipp, F. Noll, K. Eberl, K. Syassen, and F. Phillipp, *J. Electron. Mater.* **25**, 3 (1996).
- [12] S. P. DenBaars, C. M. Reaves, V. Bressler-Hill, S. Varma, W. H. Weinberg, and P. M. Petroff, *J. Cryst. Growth* **145**, 721 (1994).
- [13] N. Carlsson, W. Seifert, A. Petersson, P. Castrillo, M. E. Pistol, and L. Samuelson, *Appl. Phys. Lett.* **65**, 3093 (1994).
- [14] J. Ahopelto, A. A. Yamguchi, K. Nishi, A. Usui, and H. Sakaki, *Jpn. J. Appl. Phys. Part 2* **32**, L32 (1993).
- [15] Y. Nabetani, K. Sawada, Y. Fukukawa, A. Wakahara, S. Noda, A. Sasaki, *J. Cryst. Growth* **193**, 470 (1998).
- [16] K. Eberl, A. Kurtenbach, M. Zundel, N. Y. Jin-Phillipp, F. Phillipp, A. Moritz, R. Wirth, and A. Hangleiter, *J. Cryst. Growth* **175/176**, 702 (1997).
- [17] T. Riedl, E. Fehrenbacher, A. Hangleiter, M. K. Zundel, and K. Eberl, *Appl. Phys Lett.* **73**, 3730 (1998).
- [18] Y. M. Manz, O. G. Schmidt, and K. Eberl, *Appl. Phys. Lett.* **76**, 3343 (2000).
- [19] J. Porsche, M. Ost, F. Scholz, A. Fantini, F. Philipp, T. Riedl, and A. Hangleiter, *IEEE J. Select. Topic Quantum Electron.* **6**, 482 (2000).
- [20] G. Walter, N. Holonyak, Jr., J. H. Ryou and R. D. Dupuis, *Appl. Phys. Lett.* **78**, 26, 4091 (2001).
- [21] J. H. Ryou, R. D. Dupuis, G. Walter, D. A. Kellogg, N. Holonyak, Jr., D. T. Mathes, R. Hull, C. V. Reddy, and V. Narayanamurti, *Appl. Phys. Lett.*, **79**, 4091 (2001).
- [22] J. H. Ryou, R. D. Dupuis, D. T. Mathes, R. Hull, C. V. Reddy, and V. Narayanamurti, *Appl. Phys. Lett.* **78**, 3526 (2001).
- [23] J. H. Ryou, R. D. Dupuis, C. V. Reddy, V. Narayanamurti, D. T. Mathes, R. Hull, A. Mintairov, and J. L. Merz, *J. Electron. Mat.* **30**, 471 (2001).
- [24] G. Walter, N. Holonyak, Jr., J. H. Ryou and R. D. Dupuis, *Appl. Phys. Lett.* **79**, 3215 (2001).